Heat Production and Growth Kinetics of *E. coli* K12 from Flow Calorimetric Measurements on Chemostat Cultures

H. P. Leiseifer*

Abteilung Biophysikalische Chemie – ICH, Kernforschungsanlage Jülich GmbH, Postfach 1913, D-5170 Jülich 1, Bundesrepublik Deutschland

Z. Naturforsch. **44c,** 1036–1048 (1989); received November 28, 1986/August 8, 1989

Glucose Limited Aerobic Chemostat Culture, Steady State Heat Production, Specific Growth Rate, First Order Reaction Kinetics

The heat production of *E. coli* K12 growing aerobically in glucose limited chemostat cultures is determined in the range of specific growth rates μ (= dilution rates D) from 0.058 h^{-1} to 0.852 h^{-1} for two different glucose concentrations S_e in the instream of the chemostat, namely $S_{e1} = 0.3182$ $g \cdot l^{-1}$ and $S_{e2} = 0.6364$ $g \cdot l^{-1}$. Heat production $\dot{Q}$ and biomass production P per unit of culture volume show well correlated patterns for S_{e1} and S_{e2}. For S_{e1} the highest value $\dot{Q}$ actually measured is $443 \cdot 10^{-3}$ $W \cdot l^{-1}$ at $D = 0.74$ h^{-1} with $P = 0.068$ $g \cdot l^{-1} \cdot h^{-1}$; and for S_{e2} $593 \cdot 10^{-3}$ $W \cdot l^{-1}$ at $D = 0.497$ h^{-1} with $P = 0.108$ $g \cdot l^{-1} \cdot h^{-1}$.

Heat production $\dot{Q}_B$ per unit of biomass appears to be independent of S_e at least up to $D = 0.5$ h^{-1}. At higher D there is strong indication that $\dot{Q}_B$ possesses a real maximum. The highest value of $\dot{Q}_B$ actually measured is 4.8 $W \cdot g^{-1}$ at $D = 0.74$ h^{-1}.

For S_{e1} and S_{e2} there were significantly higher specific growth rates verified in chemostat culture than $\mu_{max}^{Batch} = 0.717$ h^{-1} which is the maximum specific growth rate in comparable, unlimited batch cultures.

The real maximum of $\dot{Q}_B$ is estimated to be in the vicinity of μ_{max}^{Batch}.

This suggests the hypothesis of a maximum principle for the growth in batch culture.

For S_{e1} a closed analytical expression is derived for the relationship between μ and the substrate concentration S. $\mu[S]$ features a S-shaped characteristic with $\mu_{max}^{Chemostat} = 0.905$ h^{-1}; 1/2 $\mu_{max}^{Chemostat}$ is reached at $S = 2.85 \cdot 10^{-3}$ $g \cdot l^{-1}$.

Three basic parameters which characterize the overall metabolism of the cells, namely the heat released per unit of substrate consumed, Q_S, the effective yield of biomass, Y_{eff}, and $\mu_{max}^{Chemostat}$ are identified to depend on S_e.

1. Introduction

Analogous to classical methods (*e.g.* [1, 2]), the time course of the heat production of bacterial cells leaving the steady state of a chemostat culture is recorded by performing calorimetric measurements at different, constant flow rates through the calorimetric measuring tube of a calorimeter-fermentor combination [3].

By employing a linear reaction kinetic model for the substrate consumption of the cells on their way from the chemostat to the measuring tube, two basic informations are drawn from the time course recordings.

First, the heat production which corresponds to flow rate "∞" is identified with the heat production $\dot{Q}$ of the culture *in the chemostat.*

Second, the resulting first order reaction constants are evaluated to yield the relationship between the specific growth rate of the culture and the substrate (glucose) concentration in the medium.

For the theoretical and numerical problems associated with the approach outlined above, a detailed mathematical framework is given.

2. Experimental Set-Up

2.1 Calorimeter-Fermentor combination

The combination consists of a fermentor (type "Biostat", Fa. Braun Melsungen AG, W. Germany) which is connected to a twin flow through calorimeter (type "Microcalorimetry System 2107", LKB Produkter AB, Sweden).

The set-up is operated in a so-called "twin flow mode": whilst culture fluid (sample) is routed through one of the calorimetric measuring tubes, steril medium (reference) is routed through the other one. Before entering the measuring tubes sample and reference each pass the same prethermostatic

* Present address: ESTEC (European Space Research and Technology Centre), P.O. Box 299, 2200 AG Noordwijk, The Netherlands.

Verlag der Zeitschrift für Naturforschung, D-7400 Tübingen
0341–0382/89/1100–1036 $ 01.30/0

water bath which is controlled by a PTC 40 (Tronac Inc. Orem/Utah, U.S.A.).

Since the thermopiles of the measuring tubes are connected in opposition, thermal disturbances cancel out.

Via pinch cocks it is possible to select the modes "Reference against Reference" (mode I) or "Reference against Sample" (mode II). The difference between the corresponding calorimeter signals constitutes the measuring signal.

A detailed description of the set-up is given in [3].

For reasons of sterility, culture fluid pumped through the calorimeter is wasted.

Measurements with the concentration $S_{e2} = 0.6364\ g \cdot l^{-1}$ were performed with a prethermostat type N3 (Fa. Gebr. Haake, Karlsruhe, W. Germany) instead of the PTC 40.

With the N3, also the routing of the water in the prethermostat was slightly modified and no additional stirrer was used.

2.2 Chemostat

The culture vessel 14 (see Fig. 1) of the set-up for batch cultures [3] has been equipped with the necessary peripherics to allow for chemostat operation.

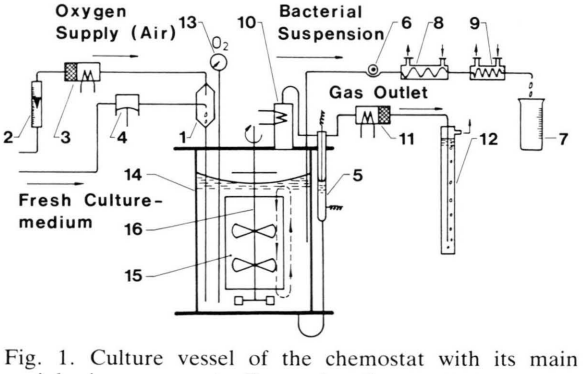

Fig. 1. Culture vessel of the chemostat with its main peripheric components. For explanation see text.

Supply of medium and oxygen is achieved by forcing droplets of medium with the air stream down the glass tube of a mixing device (1). A rota flow (2) controls the rate of oxygen supply and an electrically heated filter (3) prevents contamination of the culture. A precision membrane pump (4) assures constant flow of fresh medium into the culture vessel.

A gauge (5) which shortens two platinum electrodes if the microbial suspension exceeds a prefixed level, controls the volume of the culture *via* a peristaltic pump (6). Excess culture fluid is wasted into the measuring cylinder (7) through hot heat exchangers (8) (9), which prevent microbial infections.

For reasons of pressure compensation, the gauge (5) is connected to the outstream of the fermentor gas, the latter being cooled (10), to prevent water loss and undefined formation of water drops in (5).

The fermentor gas leaves the culture vessel through an electrically heated filter tube (11) and a water column (12) such that a pressure of ~ 1000 mm water column prevails above the culture. Determination of the dilution rate is accomplished with the measuring cylinder (7) and a precise watch.

The partial pressure of oxygen in the culture is continuously recorded by employing a polarographic electrode (13).

Mixing of the culture is achieved by a turbine stirrer system which comprises the stirrer (16) and the double walled cylinder jacket (15). The latter serves also as a heat exchanger for temperature control of the culture.

3. Methods

3.1 Calorimetric methods

The calorimetric measurements were performed as described in [3].

After the establishment of a selected steady state in the chemostat flow mode I is selected (Reference against Reference) for a fixed flow rate through the calorimeter to establish the calorimetric baseline.

Afterwards, with unchanged flow rate, mode II (Reference against Sample) is selected and the resulting constant calorimetric signal is calibrated by the application of JOULE heat.

For the same steady state of the chemostat the above procedure is repeated for several different flow rates of Reference/Sample to form a measurement sequence.

In this way the required time course record of heat productions allocated to a specific steady state of the chemostat is obtained. The above procedure has to be performed for each steady state. The parameters at hand for variation of the steady states are the dilution rate D or the concentration S_e.

3.2 Microbial methods

All experiments were performed with *Escherichia coli* strain K12, λ-lysogen [4, 5] at 37 °C.

The mineral salt medium as given in [3] was used with either $S_{e1} = 0.3182\ g \cdot l^{-1}$ or $S_{e2} = 0.6364\ g \cdot l^{-1}$ glucose as the sole carbon and energy source.

Identification of bacterial strain, contamination tests, precultivation, sterilization of apparatus/medium, determination of dry weight and optical density were done as in [3] and [4] respectively.

Fig. 2 and 3 show typical time records of heat production starting from inoculation up to the establishment of the steady state obtained in some pre-experiments ($T = 29\ °C$, $S_e = 1.2728\ g \cdot l^{-1}$). Furthermore, the time records of the oxygen partial pressure in the culture proved to be strongly correlated to the heat production, similar to the situation in batch culture [3]. Therefore, on routine basis, the establishment of the steady state was verified by checking the constancy of the oxygen partial pressure signal on the recorder.

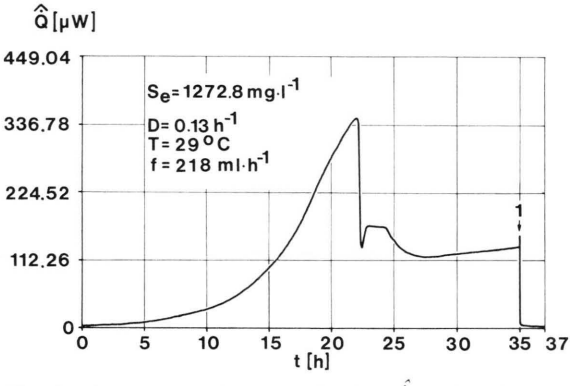

Fig. 2. Time record of heat production $\dot{Q}$ in the calorimetric measuring tube after inoculation at $t = 0$ of an already (sterile) operating chemostat and calorimeter in flow mode II. At 1 flow mode I is selected to check for the stability of the baseline. f denotes the flow rate through the calorimeter.

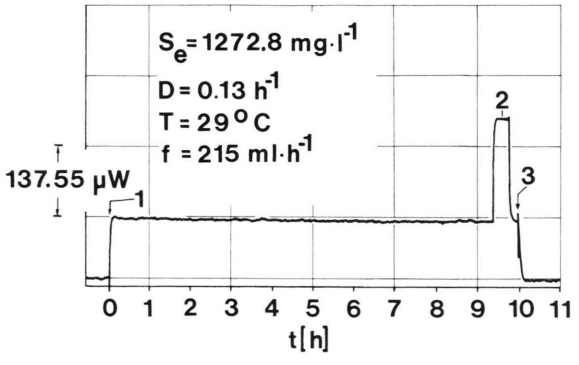

Fig. 3. Heat production $\dot{Q}$ after establishment of steady state. 1: Switching from "Reference against Reference" to "Reference against Sample". 2: Calibration by means of JOULE heat. 3: Selection of "Reference against Reference". f denotes the flow rate through the calorimeter.

4. Results

Representative examples of calorimetric measurement sequences are depicted in Fig. 4 to 7.

With S_{e1} a total of eight sequences, with S_{e2} a total of twelve sequences were carried out.

The solid curves represent the functional relationship

$$\dot{Q}_f = \frac{\dot{Q} \cdot f}{B \cdot V_M} \left\{ \exp\left[B \frac{V_1}{f}\right] - \exp\left[B \frac{V_2}{f}\right] \right\}. \quad (4\text{-}1)$$

Here f denotes the flow rate through the calorimeter and $\dot{Q}_f$ the volume specific heat production (Watt per liter of culture volume) as measured at that given f.

V_1 means the volume V_M of the measuring tube of the calorimeter plus the volume V_2 of the connection tube to the chemostat. B stands for the first order kinetic constant and $\dot{Q}$ for the volume specific heat production of the chemostat culture. B and $\dot{Q}$, both have been determined to give the best fit to the points of each measurement sequence.

The values for $\dot{Q}$ have been introduced into the figures as straight horizontal lines identified by arabic numbers. Prior to carrying out the fit, the

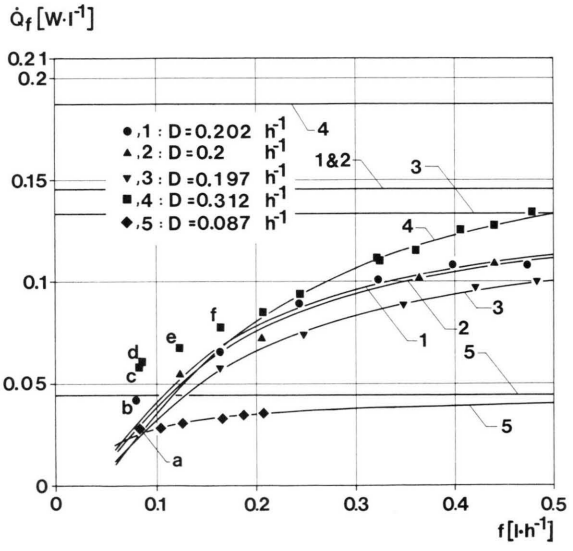

Fig. 4. Heat production $\dot{Q}_f$ *versus* flow rate f through the calorimeter for different dilution rates D. $S_e = 0.3182\ g \cdot l^{-1}$, $T = 37\ °C$.

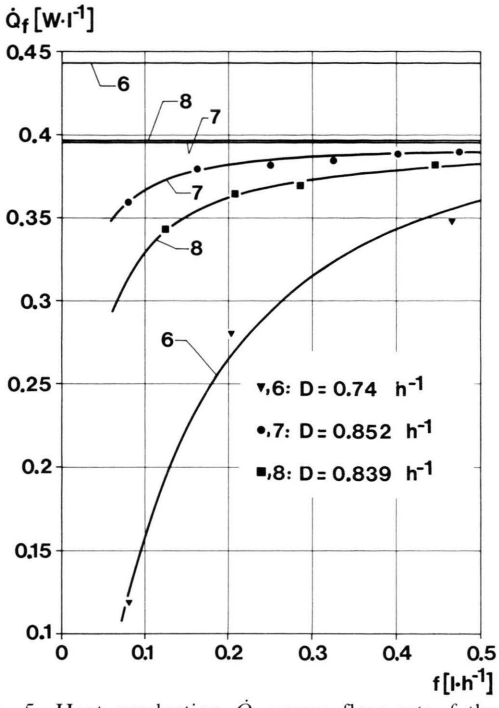

Fig. 5. Heat production $\dot{Q}_f$ *versus* flow rate f through the calorimeter for different dilution rates D. $S_e = 0.3182$ g·l^{-1}, $T = 37$ °C.

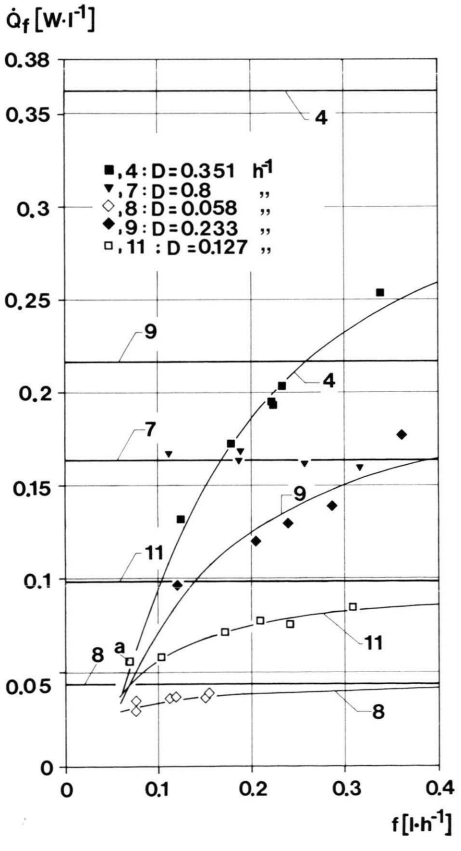

Fig. 6. Heat production $\dot{Q}_f$ *versus* flow rate f through the calorimeter for different dilution rates D. $S_e = 0.6364$ g·l^{-1}, $T = 37$ °C.

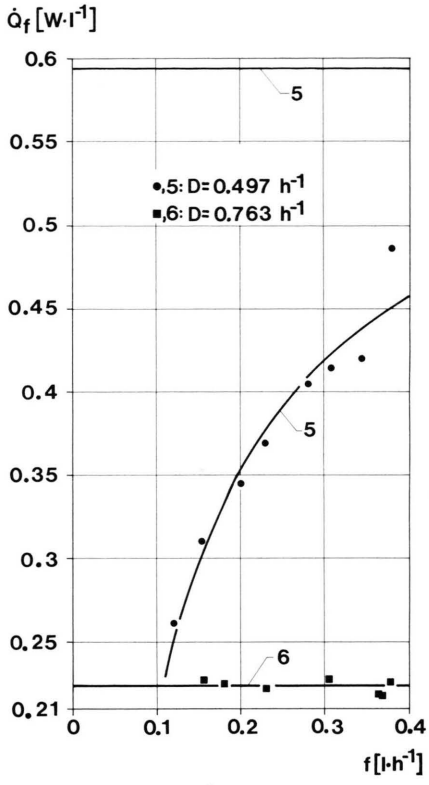

Fig. 7. Heat production $\dot{Q}_f$ *versus* flow rate f through the calorimeter for different dilution rates D. $S_e = 0.6364$ g·l^{-1}, $T = 37$ °C.

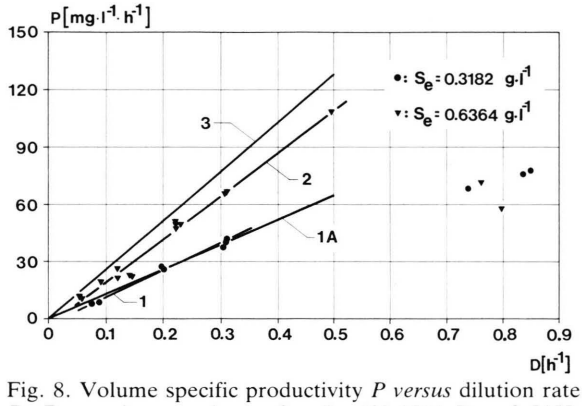

Fig. 8. Volume specific productivity P *versus* dilution rate D. Regressions used are: S_{e1}: $P = 139.8584\ D - 2.5455$, $r = 0.991$ (Line 1). S_{e2}: $P = 223.9144\ D - 3.3944$, $r = 0.993$ (Line 2). Line 1A: distribution free fit. Line 3: expected values for S_{e2}.

measurement points were checked against significant deviations from the first order regime at low flow rates and if necessary rejected (points indicated by small latin characters in the Fig. 4 and 6, details see chapter 6).

In addition to the calorimetric measurements, the formation of biomass in the chemostat was measured by determining the steady state dry mass $\bar{N}$ per liter of culture volume. Fig. 8 shows the results as volume specific productivity P *versus* dilution rate, where P is defined as

$$P = \bar{N} \cdot D.$$

The values for $\bar{N}$ used for further evaluation were either determined from sampling immediately after the calorimetric runs or from linear regression of P, *i.e.* lines 1 and 2 in Fig. 8.

The numerical results of all measurements are summarized in Tables I and II.

In Table I, the calorimetric measurement sequence 4, and in Table II the sequences 1, 3, 4, 5 and 8 contain measurement points taken on two subsequent days.

All other sequences were taken within a 12 h period throughout one day.

$\dot{Q}_B$ denotes the biomass specific heat production, *i.e.*

$$\dot{Q}_B = \dot{Q} / \bar{N}.$$

For sequences 6 and 7 in Table II there was no evidence for $B < 0$, rather the case $B = 0$ was anticipated.

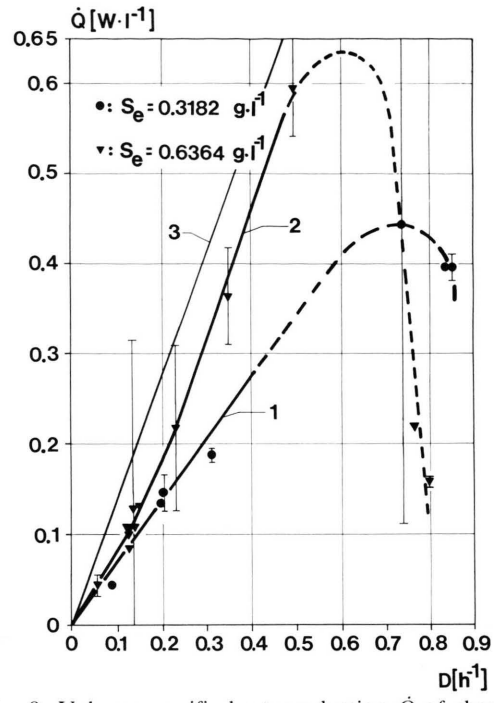

Fig. 9. Volume specific heat production $\dot{Q}$ of chemostat culture *versus* dilution rate D. 1 and 2: distribution free fit. 3: expected values for S_{e2}.

Table I. Results of calorimetric and chemostat measurements, $S_e = 0.3182\ g \cdot l^{-1}$.

No. of sequence	D [h^{-1}]	B [h^{-1}]	$\dot{Q}$ [$W \cdot l^{-1}$]	$\bar{N}$ [$g \cdot l^{-1}$]	$\dot{Q}_B$ [$W \cdot g^{-1}$]
1	0.202	− 76 ± 24	0.146 ± 0.019	0.127	1.15 ± 0.16
2	0.200	− 80 ± 41	0.146 ± 0.037	0.127	1.15 ± 0.16
3	0.197	− 86 ± 14	0.133 ± 0.01	0.127	1.05 ± 0.09
4	0.312	−102.6 ± 8.7	0.188 ± 0.008	0.132	1.42 ± 0.09
5	0.087	− 28 ± 8.9	0.044 ± 0.004	0.111	0.402 ± 0.04
6	0.740	− 62 ± 97	0.443 ± 0.33	0.092	4.8 ± 3.6
7	0.852	− 4.4 ± 1.0	0.395 ± 0.004	0.091	4.35 ± 0.21
8	0.839	− 11 ± 3.9	0.396 ± 0.013	0.09	4.4 ± 0.25

All given uncertainties refer to a 95% confidence level. For further details see chapter 6.6.

5. Discussion

5.1 Heat production of chemostat culture

The volume specific heat production $\dot{Q}$ *versus* the dilution rate D is shown in Fig. 9.

For each of the concentrations, namely S_{e1} in the range of $0 \leq D \leq 0.35\ h^{-1}$ (solid line 1) and for S_{e2} in the range of $0 \leq D \leq 0.5\ h^{-1}$ (solid curve 2) a rough fit with equal number of measurement points on either side (distribution free fit) including the origin is depicted.

At higher dilution rates (dashed) there is strong indication for the existence of a maximum for each of the two concentrations. A qualitative understanding of this behaviour is achieved by introducing the heat liberated per unit mass of metabolized energy source (glucose), Q_S, and two additional, rather general assumptions on Q_S and the specific growth rate μ.

As to Q_S, this entity is defined *via* the glucose balance of the chemostat which, employing $\mu = D$ in steady state [6-8] leads to

$$\dot{Q} = Q_S\,(\bar{S} - S_e)\,\mu,\ Q_S \leq 0,\ \mu = D. \qquad (5\text{-}1)$$

The assumptions are:

(i) $\mu = \mu[S]$ is a function of the actual substrate concentration and as such, increases strictly monotonously in S with $0 \leq \mu \leq \mu_{max}^{Chemostat}$ and $\mu[S = 0] = 0$.

$\mu_{max}^{Chemostat}$ represents the maximum specific growth rate as verified in chemostat culture.

(ii) $Q_S = Q_S[\mu]$ is continuous and bounded in the interval $0 \leq \mu \leq \mu_{max}^{Chemostat}$.

The first assumption is suggested by measurements in batch culture [6, 11] as well as by the findings reported in chapter 5.2. The second one states the existence of an exothermic process over the entire range of growth rates without jumps and singularities.

(5-1) together with (i) und (ii) implies that $\dot{Q} \geq 0$ as a function of $D = \mu$ possesses at least one extremum in the interval $[0, \mu_{max}^{Chemostat}]$.

Table II. Results of calorimetric and chemostat measurements, $S_e = 0.6364\ g \cdot l^{-1}$.

No. of sequence	D [h^{-1}]	B [h^{-1}]	$\dot{Q}$ [$W \cdot l^{-1}$]	$\bar{N}$ [$g \cdot l^{-1}$]	$\dot{Q}_B$ [$W \cdot g^{-1}$]
1	0.150	−46	0.131	0.201	0.652
2	0.139	−38 ± 140	0.128 ±0.186	0.199	0.643 ±0.935
3	0.139	−32 ± 21	0.108 ±0.028	0.199	0.542 ±0.141
4	0.351	−82 ± 20	0.363 ±0.054	0.214	1.69 ±0.26
5	0.497	−63 ± 18	0.593 ±0.054	0.217	2.73 ±0.37
6	0.763	0	0.224 ±0.004	0.093	2.4 ±0.12
7	0.800	0	0.164 ±0.005	0.072	2.27 ±0.13
8	0.058	−14 ± 17	0.044 ±0.012	0.165	0.265 ±0.072
9	0.233	−67 ± 60	0.217 ±0.092	0.209	1.04 ±0.44
10	0.122	−28 ± 10	0.108 ±0.011	0.196	0.551 ±0.062
11	0.127	−34 ± 13	0.099 ±0.011	0.197	0.503 ±0.062
12	0.128	−17 ± 8	0.083 ±0.008	0.197	0.421 ±0.044

Similar considerations can be applied to the productivity P.

Introducing the effective yield Y_{eff} according to

$$P = \bar{N} \cdot D = Y_{eff} (S_e - \bar{S}) D, \; D = \mu. \qquad (5\text{-}2)$$

and requiring Y_{eff} also to be bounded and continuous, P *versus* D should possess at least one extremum as well. Looking at the experimental results as depicted in Fig. 8 and 9, there is indeed agreement between the measurements and the above arguments: $\dot{Q}$ and P each indicate the existence of at least one maximum for each S_e although less evident for P at S_{e2}. Furthermore, the relationship between the slopes of the lines 1 and 2 (for $\dot{Q}$, Fig. 9) and lines 1 A and 2 (for P, Fig. 8) deserves attention. Generally, substrate concentrations of chemostat cultures for specific growth rates smaller than the maximum one of comparable batch cultures are expected to be very low [11]. In our case therefore, we assume the approximation

$$| \bar{S} - S_e | \approx S_e \qquad (5\text{-}3)$$

to be valid in the range $0 \leq D \leq 0.35\ h^{-1}$.

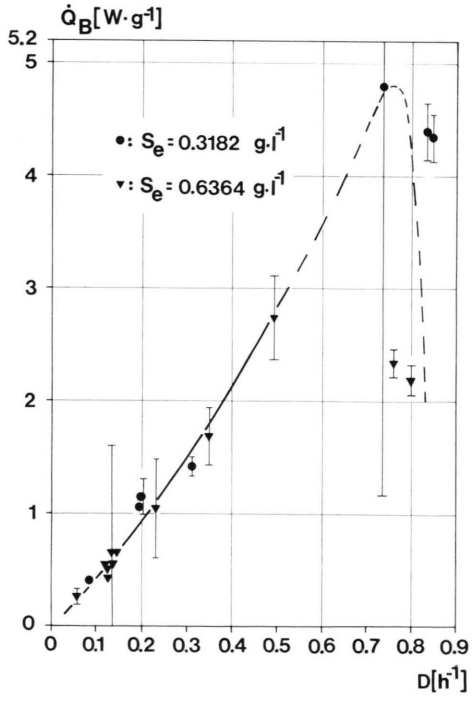

Fig. 10. Biomass specific heat production $\dot{Q}_B$ of chemostat culture *versus* dilution rate D.

Feeding (5-3) into (5-1) and (5-2) respectively we conclude that for fixed D at low dilution rates $\dot{Q}$ and P should be proportional to S_e.

This however is obviously not confirmed by the measurements. In Fig. 9 and 8, lines 3 represent the "theoretical" slopes for S_{e2} with the values for S_{e1} as reference.

For $\dot{Q}$ as well as for P the measured values appear to be lower than expected.

This in turn leads to the conclusion that the two quantities Q_S and Y_{eff}, both characterizing the overall metabolism of the cells depend on S_e with equal directions of variation.

This suggests, that an expression which contains the ratio Q_S/Y_{eff} should be studied.

Such an expression is the biomass specific heat production $\dot{Q}_B$, *i.e.*

$$\dot{Q}_B = \frac{\dot{Q}}{\bar{N}} = \frac{Q_S (\bar{S} - S_e) D}{Y_{eff} (\bar{S}_e - S)} = - \frac{Q_S}{Y_{eff}} D. \qquad (5\text{-}4)$$

Apart from its practical meaning, *e.g.* for the thermal design of fermentors, $\dot{Q}_B$ is a simple expression which only contains entities which are intimately tied to the overall metabolism of the cell.

A plot of $\dot{Q}_B$ *versus* D is shown in Fig. 10. At least for dilution rates up to $0.5\ h^{-1}$, the distribution free fit (solid line) shows that the variations of Q_S and Y_{eff} as a function of S_e are of equal magnitude and direction.

We take this as a guideline for our further discussion and additionally pay attention to the fact that in chemostat cultures considerable, higher specific growth rates were verified than in batch culture, a feature also reported by others [5, 9].

In the present case we find $\mu_{max}^{Batch} = 0.717\ h^{-1}$ [3] compared with the highest value measured which was $0.852\ h^{-1}$ ($S_e = S_{e1}$) and a computed value of $\mu_{max}^{Chemostat} = 0.9056\ h^{-1}$ (for S_{e1}, see chapter 5.2).

Despite the few measurements available so far, Fig. 10 is taken to indicate a maximum of $\dot{Q}_B$ around $D = 0.75\ h^{-1}$, which is in the close vicinity of μ_{max}^{Batch} (dashed line). This behaviour of $\dot{Q}_B$ at higher dilution rates is taken to formulate the following conjecture concerning a maximum principle for the growth in batch culture:

"Let the species as studied in chemostat culture grow in batch culture under comparable conditions; *i.e.* equal minimal medium, oxygen supply, type of carbon and energy source (glucose) and temperature, with carbon and energy source in excess. The

species will then grow at that specific growth rate, at which the biomass specific heat production in chemostat culture attains a maximum value."

Since $\dot{Q}_B$ is the sum of all heat fluxes associated with the irreversible processes in the living cell, $\dot{Q}_B$ can be taken as a measure of the biomass specific metabolic activity of the organism.

Based on this, a more general, but also more speculative formulation of the above conjecture can be given:

"During the exponential phase of growth in batch culture the present species adjusts its specific growth rate such that under the given conditions the associated biomass specific activity attains a maximum value."

5.2 *The relationship between μ and S*

Starting point is the relationship

$$B = \frac{\partial \mu}{\partial S}(S - S_e) + D, \mathrm{D} = \mu \tag{5-5}$$

which is interpreted as a differential equation of μ in S (see chapter 6.5).

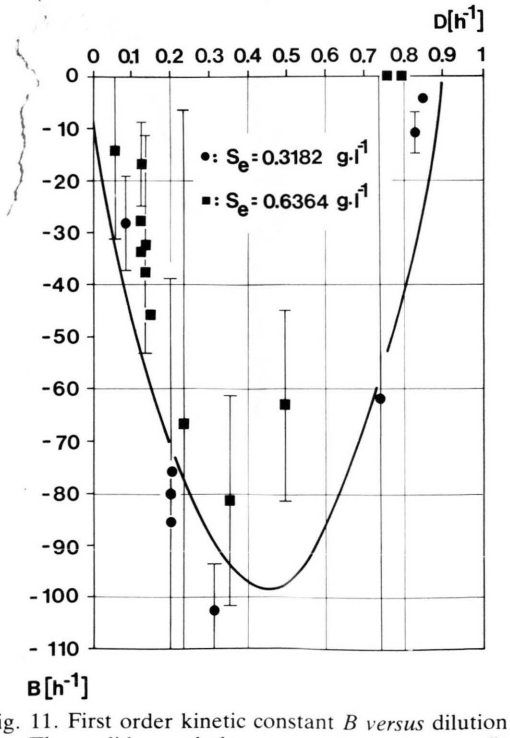

Fig. 11. First order kinetic constant B *versus* dilution rate D. The solid parabola represents a coarse fit for $S_e = 0.3182\ \mathrm{g \cdot l^{-1}}$.

The integration of (5-5) requires B to be known as a function of μ, which is obtained from a plot of B *versus* D (Fig. 11). In the present case, the integration was carried out only for $S_e = S_{e1}$ since in that case a simple if even rough fit for B *versus* D could be applied.

The curve in Fig. 11 follows the equation

$$B = aD^2 + bD + c \tag{5-6}$$

with B and D given in $\mathrm{h^{-1}}$.

The ordinate section c has been determined independently by linear regression involving all measurements up to $D = 0.312\ \mathrm{h^{-1}}$ (*i.e.* sequences 1 to 5), with correlation coefficient $r = 0.9445$ to yield

$$c = -8.537. \tag{5-7}$$

Subsequently, all eight measured values (*i.e.* sequences 1 to 8) were subjected to a linear regression of

$$\frac{B - c}{D} = aD + b \tag{5-8}$$

with c according to (5-7), leading to

$$\left.\begin{aligned} a &= 461.96 \\ b &= -407.936 \end{aligned}\right\} \tag{5-9}$$

with $r = 0.9151$.

The solution of (5-5), utilizing the numerical values (5-7) and (5-9) is given in chapter 6.5, and it reads

$$\mu[S] = \frac{\left\{\left(\frac{S_e - S}{S_e}\right)^{2\gamma} - 1\right\}(E - \gamma)}{a\left\{1 - \left(\frac{S_e - S}{S_e}\right)^{2\gamma}\left(\frac{E - \gamma}{E + \gamma}\right)\right\}}, \tag{5-10}$$

$0 \leq S \leq S_e$;

with:

$$\left.\begin{aligned} \gamma &= \sqrt{E^2 - ac} = 213.895 \\ E &= \frac{b - 1}{2} = -204.468 \end{aligned}\right\} \tag{5-11}$$

and μ[S] given in $\mathrm{h^{-1}}$.

Equation (5-10) gives the desired growth kinetic relationship for each specific concentration S_e.

$\mu = \mu_{max}^{Chemostat}$ is reached for $S = S_e$, *i.e.*

$$\mu_{max}^{Chemostat} = -\frac{E - \gamma}{a} = 0.9056\ \mathrm{h^{-1}}. \tag{5-12}$$

According to (5-12), $\mu_{max}^{Chemostat}$ is solely determined by the parameters of the relationship between B and D.

Consequently, a possible dependence of $\mu_{max}^{Chemostat}$ on S_e should show up in a dependence of $B[D]$ on S_e. In fact, such a dependency is suggested by the measurements performed with S_{e2} (Fig. 11).

Accordingly, beside Q_S and Y_{eff}, a third essential parameter of the overall metabolism, $\mu_{max}^{Chemostat}$ is expected to depend on S_e.

Equation (5-10) with the values from (5-11) is plotted in Fig. 12, curve 1.

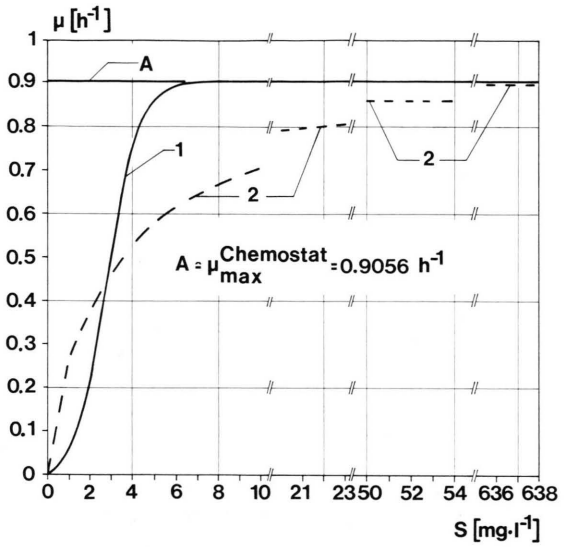

Fig. 12. Growth kinetics in chemostat culture: relationship between specific growth rate μ and substrate concentration S in the medium. Curve 1: Evaluation of calorimetric measurements with $S_e = 0.3182\ g \cdot l^{-1}$. Curve 2: MICHAELIS MENTEN kinetics with saturation level $\mu_{max}^{Chemostat}$ and K_s defined as $\mu[K_s] = 1/2\ \mu_{max}^{Chemostat}$.

The graph is characterized by the existence of an inflection point and an extremly rapid increase towards the saturation level. This is in complete contrast to a growth kinetics of MICHAELIS MENTEN type [10, 11] *i.e.*

$$\mu[S] = \mu_{max} \frac{S}{K_S + S} \tag{5-13}$$

with K_S being the substrate concentration at which μ reaches half the maximum value μ_{max}.

Employing the values

$$\mu_{max} = \mu_{max}^{Chemostat} = 0.9056\ h^{-1} \tag{5-14}$$

and a graphically determined value (from curve 1) which amounts to

$$K_S = 2.85\ mg \cdot l^{-1}, \tag{5-15}$$

curve 2 (dashed) has been computed to illustrate the fundamental difference between the two growth kinetics.

5.3 Summary and overall assessment

The combination of a flow through calorimeter and a chemostat proves to be a valid tool to determine both chemostat culture heat production as well as growth kinetics.

The volume specific heat production $\dot{Q}$ as a function of dilution rate D shows an almost linear, monotonously increasing behaviour at low dilution rates, and a maximum at higher ones.

Both features are deducible from basic general assumptions on the metabolism of the cells and are also strictly correlated to the behaviour of the volume specific biomass production P. $\dot{Q}$ and P are also strictly correlated to the glucose concentration S_e in the instream of the chemostat which is interpreted as an S_e dependency of the basic metabolic parameters Q_S (heat liberated per unit of consumed glucose) and Y_{eff} (effective yield of biomass).

The biomass specific heat production, $\dot{Q}_B$, which contains the ratio of Q_S and Y_{eff} increases at lower dilution rates monotonously whilst dropping sharply at higher ones. The maximum is estimated to be at $\mu = 0.75\ h^{-1}$ which is near $\mu = \mu_{max}^{Batch} = 0.717\ h^{-1}$, the specific growth rate determined in comparable, unlimited batch culture.

This suggests the formulation of a maximum principle for growth in batch culture: the exponential phase of growth in batch culture is characterized by a specific growth rate at which the biomass specific heat production reaches the maximum possible value under the given conditions.

The existence of a maximum of $\dot{Q}_B[D]$ is not deducible from basic assumptions as in the case of the maxima of $\dot{Q}$ and P. Furthermore, at high D's we suffer from a low number of measurements, and in one case ($D = 0.74\ h^{-1}$) from the extreme broad confidence intervall (although here driven by having only 1 (!) residual degree of freedom).

Consequently, the stated maximum principle must be considered only as a working hypothesis for the time being. However, despite its speculative character, it is found attractive enough to deserve the effort of further experimental investigation. The relationship between the specific growth rate and the substrate concentration S in the medium μ[S], is obtained

in closed, analytical form by integrating a differential equation associated with the first order kinetic constant B of the calorimetric measurement sequences.

μ[S] is found to possess an S-shaped characteristic which is *e.g.* in contrast to the MICHAELIS MENTEN kinetics with its concave shape. Apart from this fundamental difference, μ[S] as determined here fits well into the expected picture of having a rather steep increase towards the saturation level $\mu_{max}^{Chemostat}$.

Further, $\mu_{max}^{Chemostat}$ appears to be solely dependent on the parameters of $B = B[D]$.

Due to the dependency of B on S_e, $\mu_{max}^{Chemostat}$, as well as Q_S and Y_{eff} is considered to be S_e dependent.

The consequence of this finding, especially on the maximum principle, can only be evaluated after further, more detailed experimental investigations together with the build-up of dedicated, expanded mathematical tools.

6. Mathematical Framework for the Evaluation of Calorimetric Measurement Sequences

6.1 Linearization of growth kinetic equations

Let N be the concentration of biomass (gramms dry weight per liter), S the concentration of glucose and Y_{eff} the effective yield as defined by the equation

$$\bar{N} = Y_{eff}(S_e - \bar{S}). \tag{6-1}$$

The bars denote the time independent values of N, S in the steady state of the chemostat culture. S_e stands for the constant concentration of the glucose in the fresh medium of the chemostat.

A volume element leaving the chemostat to reach the calorimetric measuring tube is considered to be a batch culture, the growth of which is governed by the equations

$$\frac{d}{dt} N[t] = \dot{N} = \mu[S]\, N[t] \tag{6-2}$$

$$\frac{d}{dt} S[t] = \dot{S} = -Y_{eff}^{-1} \dot{N} \tag{6-3}$$

with the initial conditions

$$N_{t=0} = \bar{N} \tag{6-4}$$

$$S_{t=0} = \bar{S}. \tag{6-5}$$

The [ ]-brackets contain the independent variable which the corresponding function acts upon.

μ[S] is the specific growth rate of the culture as a function of the substrate concentration S. (6-2) and (6-3) lead to

$$\frac{d}{dt}\left\{N[t] + Y_{eff}\, S[t]\right\} = 0 \tag{6-6}$$

with the solution

$$N[t] + Y_{eff}\, S[t] = \text{const.} = \theta, \tag{6-7}$$

where Y_{eff} is taken to be time independent.

Determining θ by using (6-1) and the initial conditions (6-4) and (6-5), the equations (6-2) and (6-3) can be transformed into a differential equation in S, namely

$$\dot{S} = \mu[S]\,(S - S_e) = F[S]. \tag{6-8}$$

Equation (6-8) is linearized by employing the transformation:

$$S[t] = \bar{S} + y_s[t] \tag{6-9}$$

which defines the deviation $y_s[t]$ of the substrate concentration from its steady state value $\bar{S}$.

From (6-9) we arrive at

$$\dot{S} = \dot{y}_s = \mu[\bar{S} + y_s]\,(\bar{S} + y_s - S_e) = F[\bar{S} + y_s]. \tag{6-10}$$

The linear part of the corresponding TAYLOR series reads:

$$F[\bar{S} + y_s] = F\Big|_{\bar{S}} + \frac{\partial F}{\partial S}\Big|_{\bar{S}} \cdot y_s. \tag{6-11}$$

The application of (6-11) to (6-8) yields the desired linearized form of (6-8), namely

$$\dot{y}_s = D(\bar{S} - S_e) + \left\{\frac{\partial \mu}{\partial S}\Big|_{\bar{S}}(\bar{S} - S_e) + D\right\} y_s \tag{6-12}$$

or

$$\dot{y}_s = A + B\, y_s \tag{6-13}$$

with

$$A = D(\bar{S} - S_e) \tag{6-14a}$$

$$B = \frac{\partial \mu}{\partial S}\Big|_{\bar{S}} (\bar{S} - S_e) + D. \tag{6-14b}$$

In (6-12) the relationship $\mu[S{=}\bar{S}] = D$ has been used, where D denotes the dilution rate of the chemostat in the steady state.

(6-13) leads to the basic expression for the time dependence of S after leaving the steady state of the chemostat:

$$S[t] = \frac{A}{B}\,(\exp[Bt] - 1) + \bar{S}. \tag{6-15}$$

6.2 Measurement of first order reaction kinetics with the flow calorimeter

Estimation of the REYNOLDS number shows that for the given range of flow rates the flow pattern

of the culture fluid through the calorimetric measuring tube is laminar.

In particular, the measuring tube is considered to be a heterogeneous reactor.

Thus, for the measuring tube the steady state glucose balance for a given fixed flow rate f reads:

$$\dot{S}_f = \frac{S_{t=t_l} - S_{t=t_e}}{V_M} f, \tag{6-16}$$

where t_e and t_l denote the points of time at which a volume element of culture fluid enters, or respectively leaves, the measuring tube.

By inserting (6-13) into (6-16) we get

$$\dot{S}_f = \frac{A \cdot f}{V_M \cdot B} \left\{ \exp\left[B \frac{V_1}{f} \right] - \exp\left[B \frac{V_2}{f} \right] \right\}. \tag{6-17}$$

V_1 means the volume V_M of the measuring tube plus the volume V_2 of the connection tube to the chemostat; $V_1 = 1.993 \times 10^{-3}$ l, $V_2 = 1.3064 \times 10^{-3}$ l.

(6-17) has the properties:

$$\lim_{B \to 0} \dot{S}_f = \lim_{f \to \infty} \dot{S}_f = A = D(\bar{S} - S_e). \tag{6-18}$$

Assuming a one to one correspondence between the substrate consumption $\dot{S}_f$ and the heat production $\dot{Q}_f$, *i.e.*

$$\dot{Q}_f = Q_S \cdot \dot{S}_f, \tag{6-19}$$

with Q_S = const. at least for each fixed S_e and D, the constant B and the heat production $\dot{Q} = \lim_{f \to \infty} \dot{Q}_f$ of the chemostat culture can be determined from the series of calorimetric measurements at different, constant flow rates for the corresponding steady state of the chemostat.

6.3 Selection of measurement points for final evaluation

The multiplication of (6-17) with Q_S and utilization of (6-18) after rearrangement yields

$$B = \frac{\dot{Q} \cdot f}{V_M \cdot \dot{Q}_f} \left\{ \exp\left[B \frac{V_1}{f} \right] - \exp\left[B \frac{V_2}{f} \right] \right\}. \tag{6-20}$$

The right hand side of (6-20) is interpreted to be an operator $\Gamma_{\dot{Q}_f,f}$ which, for a given (estimated) value of $\dot{Q}$ for each fixed value pair $(\dot{Q}_f, f)$ of the corresponding calorimetric measurement series possesses B as fix point.

$\Gamma_{\dot{Q}_f,f}$ has the property of being contracting [12], *i.e.*

$$B = \lim_{\nu \to \infty} \Gamma^{\nu}_{\dot{Q}_f,f}[B_0], \tag{6-21}$$

B_0 being a rough estimate for B.

Utilizing (6-20) and (6-21), each calorimetric measurement sequence was checked as follows.

(i) First estimations of $\dot{Q}$ and B_0 are obtained by a semilogarithmic plot of $\dot{Q}_f$ *versus* the residence time t' and an subsequent extrapolation to $t' = 0$ [3].

The residence time t' represents the time which a volume element needs to reach half of the volume of the calorimetric measuring tube after leaving the culture.

(ii) Introducing the obtained value for $\dot{Q}$ into (6-20), for each measured value pair $(\dot{Q}_f, f)$, the resulting operator $\Gamma_{\dot{Q}_f,f}$ is applied to B_0 according to (6-21).

If the $(\dot{Q}_f, f)$ strictly follow the regime derived in chapters 6.1 and 6.2, the plot of the computed B *versus* flow rates f would yield a straight horizontal line.

This criterium was employed to identify significant deviations from the first order range, *i.e.* deviations of the computed B from the horizontal, at low flow rates.

If necessary, the procedure was repeated with modified values for $\dot{Q}$.

Measurement points found to deviate significantly were not taken into account for further evaluation.

6.4 Numerical method for final determination of B and $\dot{Q}$

Solving (6-20) for $\dot{Q}_f$ leads to the equation

$$\dot{Q}_f = \frac{\dot{Q} \cdot f}{V_M \cdot B} \left\{ \exp\left[B \frac{V_1}{f} \right] - \exp\left[B \frac{V_2}{f} \right] \right\} \tag{6-22}$$

(6-22) is interpreted as a functional relationship which contains f as independent variable, $\dot{Q}_f$ being the explicitely allocated experimental measuring value and $\dot{Q}$, B as implicitely allocated measuring values which are required.

The required computational determination of the $\dot{Q}$, B is performed according to a least square standard method as described in detail in [13], therein chapter 1.2.3.2.2, pp. 52ff.

6.5 Determination of relationship between the specific growth rate μ and the substrate concentration S

Solving (6-14b) for $\left.\frac{\partial \mu}{\partial S}\right|_{\bar{S}}$ yields the equation

$$\left.\frac{\partial \mu}{\partial S}\right|_{\bar{S}} = \frac{1}{\bar{S} - S_e} (B - D), \tag{6-23}$$

with $D = \mu$.

(6-23) is considered to be a differential equation of μ in S of the form

$$\frac{d}{dS}\mu = \mathcal{F}[S]\,\mathcal{G}[\mu] \tag{6-24}$$

with

$$\mathcal{F}[S] = \frac{1}{S - S_e} \tag{6-25}$$

and

$$\mathcal{G}[\mu] = B - \mu,\ B = B[\mu] \tag{6-26}$$

The bar now has been dropped since all considerations apply to chemostat steady state conditions which are parametrically varied by D.

For the solution of (6-24) an analytical expression for $\mathcal{G}$ is required; it may be obtained from a plot of B *versus* D with a subsequent fit of the measuring points.

In view of the few data available so far, an expression of the form

$$B = a\mu^2 + b\mu + c \tag{6-27}$$

is suggested by Fig. 11.

Analysis of the possible solutions of (6-24) based on (6-27) shows that the condition

$$\mu[S = 0] = 0 \tag{6-28}$$

is a reasonable working hypothesis, implies

$$c < 0. \tag{6-29}$$

Employing (6-27) and (6-29) the integration of (6-24) is straightforward [14] and yields

$$\mu[S] = \frac{\left\{\left(\frac{S_e - S}{S_e}\right)^{2\gamma} - 1\right\}(E - \gamma)}{a\left\{1 - \left(\frac{S_e - S}{S_e}\right)^{2\gamma}\left(\frac{E - \gamma}{E + \gamma}\right)\right\}} \tag{6-30}$$

with

$$\gamma = \sqrt{E^2 - ac} \tag{6-31}$$

and

$$E = \frac{b - 1}{2}\,. \tag{6-32}$$

6.6 Considerations on measurement uncertainties

To obtain a rough estimate of the uncertainties involved the following assumptions and calculations are applicable.

6.6.1 Concentration S_e and dilution rate D

In both cases, estimations lead to mean "errors" of the mean value, expressed as standard deviation, of the order of 1% to 2%.

In all cases, there were no measurement series carried out, hence, confidence intervalls are not given.

6.6.2 Volume specific biomass N

Based on a 3% mean error of the mean value and a number of measurements of dry weight of 4, a 95% confidence intervall $u_{\bar{N}}$ is given for each value of $\bar{N}$, regardless whether $\bar{N}$ has been obtained from interpolation using Fig. 8 or not.

6.6.3 Volume specific heat production $\dot{Q}$ and first order kinetic constant B

In both cases, the standard deviations $s_{\dot{Q},B}$ as obtained from the standard method [13] were taken to determine the 95% confidence intervalls $u_{\dot{Q}}$ and u_B according to

$$u_{\dot{Q},B} = \tau\, s_{\dot{Q},B}.$$

The applicable number of degrees of freedom for τ ([13], p. 48) was n-2, n being the number of measurement points of the corresponding sequence.

In the case of sequences 6 and 7 of S_{e2}

$u_{\dot{Q}} = \frac{\tau}{\sqrt{n}} \cdot s_{\dot{Q}}$ was used.

6.6.4 Biomass specific heat production $\dot{Q}_B$

The 95% confidence intervall for $\dot{Q}_B$, $u_{\dot{Q}_B}$, was calculated according to

$$u_{\dot{Q}_B} = \sqrt{\left(\frac{u_{\dot{Q}}}{\bar{N}}\right)^2 + \left(\frac{\dot{Q}}{\bar{N}^2} \cdot u_{\bar{N}}\right)^2}.$$

Acknowledgements

This paper is addressed to Renate, Andreas and Stefan for their encouragement and patience.

The author wishes to express his thanks to Dr. Schleser, Kernforschungsanlage Jülich, for his support and valuable suggestions; and to Prof. Lamprecht, Free University of Berlin, for his careful reading of the manuscript and constructive critics.

[1] J. B. Bateman and F. J. W. Roughton, Biochem. J. **29,** 2622 (1935).
[2] G. A. Milikan, Prod. Roy. Soc. (London) A **155,** 277 (1936).
[3] H. P. Leiseifer and G. H. Schleser, Z. Naturforsch. **38c,** 259–267 (1983).
[4] H. P. Leiseifer, Strömungskalorimetrische Untersuchungen an Chemostatkulturen von Escherichia Coli, Diss. RWTH Aachen, 1981.
[5] G. H. Schleser, Die Isotopenfraktionierung des Sauerstoffs bei der Respiration, Diss. RWTH Aachen, 1977.
[6] J. Monod, Annls. Inst. Pasteur, Paris, **79,** 390 (1950).
[7] A. Novick and L. Szilard, Proc. nat. Acad. Sci. (Wash.), **36,** 708 (1950).
[8] D. Herbert, R. Elsworth, and R. C. Telling, J. gen. Microbiol. **14,** 601 (1956).
[9] K. L. Schulze and R. S. Lipe, Arch. Microbiol. **48,** 1 (1964).
[10] J. Monod, Recherches sur la croissance des cultures bacteriennes Thesis Univ. Paris, 1942.
[11] G. Schleser and H. Förstel, Jül – 912 – PC (1972).
[12] H. W. Knobloch and F. Kappel, Gewöhnliche Differentialgleichungen, B. G. Teubner, Stuttgart 1974.
[13] F. Kohlrausch, Praktische Physik, **Band 1,** 22. Auflage, B. G. Teubner, Stuttgart 1968.
[14] E. Kamke, Differentialgleichungen, I, 6. Auflage, Geest & K.-G. Portig, Leipzig 1969.